Transmission Characteristics of an FDM System Using Mach-Zehnder Filters

Kazuki Tanaka*, Isamu Wakabayashi*, Masatoshi Sano*

Electrical Engineering Department, Tokyo University of Science, 1-14-6 Kudan-kita, Chiyoda-ku, Tokyo Japan

j4311647@ed.tus.ac.jp, wakaba@ee.kagu.tus.ac.jp, sano@ee.kagu.tus.ac.jp

Abstract- **A plain representation of the amplitude transfer function using a Mach-Zehnder filter model is proposed by applying the analysis technique for a transmission type periodic branching microwave filter. A four-channel frequency division multiplexing system configuration using the Mach-Zehnder filter models is presented as an example of a multi-channel FDM system. The amplitude transfer functions for the channels of the presented system are exhibited by using the proposed representation. The calculated result of a signal to inter-channel interference ratio for the system together with a two-channel and an eight-channel FDM system are shown.**

***Keywords*-Frequency division multiplexing, Mach-Zehnder filter, Periodical branching filter, ASK, Signal to inter-channel interference ratio**

I. Introduction

The periodic branching filter was developed as a microwave multi/demultiplexers and has been used in communication satellites [1][2]. This filter consists of a first directional coupler with two input/output ports, two waveguides with a traveling wave ring type resonator attached to one side of the waveguides, and a second directional coupler with two input/output ports arranged in tandem. The authors have been investigating a method for analyzing the performance of the frequency division multiplexing (FDM) system using a periodic branching filter (PBF) without a traveling wave ring type resonator. In the operating principle of the PBF, the frequency multiplexing input signal in one input port is equally divided into two signals by the first directional coupler. After the signals pass through the two waveguides, which have different lengths, a phase difference arises between the two signals. The two signals are recombined with the mutual interference at the second directional coupler. Since the relative phase difference is frequency dependent, the transmission coefficient is also frequency dependent. Thus, the amplitude transmission characteristics change periodically depending on frequency.

A second type of filter, which is a Mach–Zehnder filter (MZF), is used as an optical filter and an intensity modulator in the optical communication applications [3]-[5]. Although the PBF and the MZF have been developed separately in the respective fields, the basic structure and the operating principle of the MZF can be thought of as being similar to those of the PBF [6].

The FDM system has contributed to the increased transmission capacity and is used in the optical communication system as, in other words, the wavelength division multiplexing system [7]-[10]. However, thus far, it is difficult to analyze the transmission characteristics for the case in which the system has a much higher number of channels.

In the present paper, we propose a plain representation of the amplitude transfer function using the MZF model by applying the analysis technique of the PBF to the MZF. Then, as an example, we present a four-channel FDM system configuration in a multi-channel FDM system and present the amplitude transfer function of the four-channel FDM system. We show the calculated result of a signal to inter-channel interference ratio of the FDM system.

II. MZF Model

A. Basic Configuration

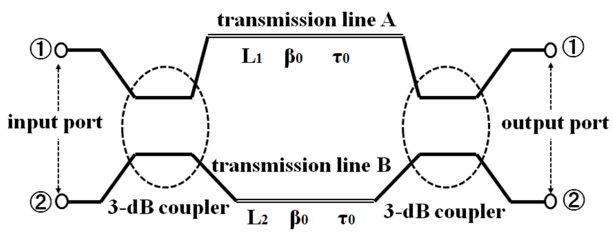

Figure 1. MZF basic configuration.

Figure 1 shows the MZF basic configuration. The MZF consists of two 3-dB couplers with two input/output ports and two optical transmission lines between the two couplers. The lengths of optical transmission lines A and B are assumed to be L_1 and L_2, respectively. Both of these lines are assumed to have a phase constant of β_0 and a delay time per unit length of τ_0 at the center radian frequency. The filter is assumed to be reciprocal and lossless with no dispersion herein. The fixed phase change and delay time are ignored. The coupling coefficient k of the two 3-dB couplers is $1/\sqrt{2}$.

The first coupler splits the input signal equally into two parts, which acquire different phase shifts, when the transmission line (arm) lengths are made different, before they interfere at the second coupler [3]. Since the relative phase shift is frequency dependent, the transmittivity is also frequency dependent. The two arm signals are recombined at the second 3-dB coupler. Thus, the transmission characteristics of the MZF, as well as those of the PBF, change periodically depending on frequency.

B. Transfer Function

The transfer function $H_{i\to o}(\omega)$ of the MZF from input port i to output port o can be expressed as follows:

$$H_{1\to1}(\omega) = \sin\frac{\beta(\omega)(L_1-L_2)}{2} e^{-j\left\{\frac{\beta(\omega)(L_1+L_2)}{2}+\frac{\pi}{2}\right\}}, \quad (1)$$

$$H_{2\to1}(\omega) = \cos\frac{\beta(\omega)(L_1-L_2)}{2} e^{-j\left\{\frac{\beta(\omega)(L_1+L_2)}{2}-\frac{\pi}{2}\right\}}, \quad (2)$$

$$H_{2\to2}(\omega) = \sin\frac{\beta(\omega)(L_1-L_2)}{2} e^{-j\left\{\frac{\beta(\omega)(L_1+L_2)}{2}+\frac{\pi}{2}\right\}}, \quad (3)$$

$$H_{1\to2}(\omega) = \cos\frac{\beta(\omega)(L_1-L_2)}{2} e^{-j\left\{\frac{\beta(\omega)(L_1+L_2)}{2}-\frac{\pi}{2}\right\}}. \quad (4)$$

The phase constant $\beta(\omega)$ is approximated to the first degree, and ΔL and L is defined as follows:

$$\beta(\omega) = \beta_0 + \tau_0(\omega - \omega_n) \quad ; n = 1,2, \quad (5)$$

$$\Delta L = L_1 - L_2, \quad (6)$$

$$L = L_1 + L_2, \quad (7)$$

$$\tau_0\Delta L = \frac{\pi}{\omega_d} = T_d, \quad (8)$$

where ω_1 and ω_2 are the center radian frequency of input ports 1 and 2, respectively, T_d is the difference in delay time between the two arms, and ω_d is the neighboring channel spacing. Finally, $\beta_0\Delta L$ is an odd multiple of π with respect to ω_1 and an even multiple of π with respect to ω_2. Substituting equations (5) through (8) into equations (1) through (4), the amplitude characteristics $A_{i\to o}(\omega)$ can be expressed as equations (9) through (12) under the condition of the identical phase shift $\theta_{i\to o}(\omega)$.

$$A_{1\to1}(\omega) = \cos\frac{\pi(\omega-\omega_1)}{2\omega_d}, \quad (9)$$

$$A_{1\to2}(\omega) = \cos\frac{\pi(\omega-\omega_2)}{2\omega_d}, \quad (10)$$

$$A_{2\to1}(\omega) = \cos\frac{\pi(\omega-\omega_2)}{2\omega_d}, \quad (11)$$

$$A_{2\to2}(\omega) = \cos\frac{\pi(\omega-\omega_1)}{2\omega_d}, \quad (12)$$

$$\theta_{1\to1}(\omega) = \theta_{1\to2}(\omega) = \theta_{2\to1}(\omega) = \theta_{2\to2}(\omega) = -\frac{\beta(\omega)L}{2} + \frac{\pi}{2}. \quad (13)$$

C. MZF Model

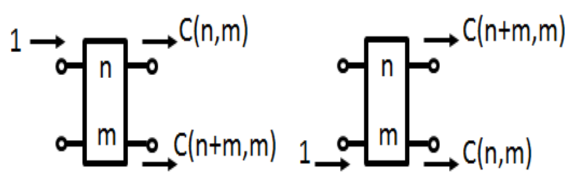

Figure 2. MZF model.

Figure 2 shows the MZF model. Based on equations (9) through (12), a plain representation of the amplitude transfer function of the MZF can be further defined as follows:

$$C(n, m) = \cos\frac{\pi(\omega-\omega_n)}{2m\omega_d}, \quad (14)$$

$$\omega_n = \omega_1 + (n-1)\omega_d, \quad (15)$$

$$n := n + 2\nu m, \quad (16)$$

where ω_n is the center radian frequency at channel n, $m\omega_d$ is the channel spacing, and ν is an integer.

III. Four-Channel FDM System

A. System Configuration

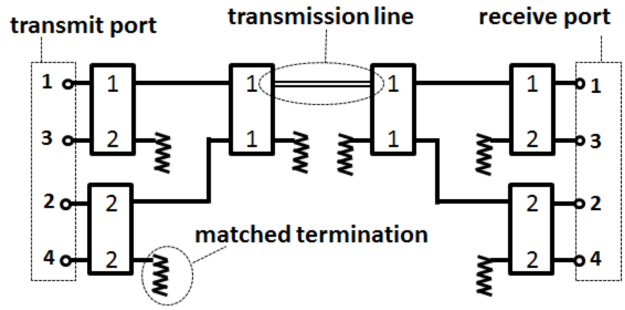

Figure 3. A four-channel FDM system configuration.

The proposed configuration of the four-channel FDM system is an example of a multichannel system, as shown in Figure 3. This system consists of three MZFs on the transmit side and three MZFs on the receive side and is reciprocal. The notched symbol represents the matched termination. The transmission line is assumed to be lossless with no dispersion.

The transfer functions between the transmit and receive ports can be expressed using equation (14) as follows:

$$H_{1\to1}(\omega) = C(1,2)C(1,1)C(1,1)C(1,2), \quad (17)$$
$$H_{1\to2}(\omega) = C(1,2)C(1,1)C(2,1)C(2,2), \quad (18)$$
$$H_{1\to3}(\omega) = C(1,2)C(1,1)C(3,1)C(3,2), \quad (19)$$
$$H_{1\to4}(\omega) = C(1,2)C(1,1)C(4,1)C(4,2), \quad (20)$$
$$H_{2\to1}(\omega) = C(2,2)C(2,1)C(1,1)C(1,2), \quad (21)$$
$$H_{2\to2}(\omega) = C(2,2)C(2,1)C(2,1)C(2,2), \quad (22)$$
$$H_{2\to3}(\omega) = C(2,2)C(2,1)C(3,1)C(3,2), \quad (23)$$
$$H_{2\to4}(\omega) = C(2,2)C(2,1)C(4,1)C(4,2), \quad (24)$$
$$H_{3\to1}(\omega) = C(3,2)C(3,1)C(1,1)C(1,2), \quad (25)$$
$$H_{3\to2}(\omega) = C(3,2)C(3,1)C(2,1)C(2,2), \quad (26)$$
$$H_{3\to3}(\omega) = C(3,2)C(3,1)C(3,1)C(3,2), \quad (27)$$
$$H_{3\to4}(\omega) = C(3,2)C(3,1)C(4,1)C(4,2), \quad (28)$$
$$H_{4\to1}(\omega) = C(4,2)C(4,1)C(1,1)C(1,2), \quad (29)$$
$$H_{4\to2}(\omega) = C(4,2)C(4,1)C(2,1)C(2,2), \quad (30)$$
$$H_{4\to3}(\omega) = C(4,2)C(4,1)C(3,1)C(3,2), \quad (31)$$
$$H_{4\to4}(\omega) = C(4,2)C(4,1)C(4,1)C(4,2). \quad (32)$$

Channels between identical port numbers are assumed to be desired channels, and channels between different port numbers are assumed to be interference channels.

B. Signal Waveform

The transmission scheme is assumed to be ASK. The transmit signal $g_{T1}(t)$ of channel 1 is represented by equation

(33). Channel 1 is assumed to be the desired channel here.

$$g_{T1}(t) = \sum_{k=-\infty}^{\infty} a_k g(t - kT)\cos\omega_1 t\,, \quad (33)$$

where a_k is the independent, and identical random variables that take 1 or 0, $g(t)$ is a rectangular pulse with unit amplitude and a pulse width of T, which is the symbol period. The frequency spectrum of a single pulse, g(t), is given as follows:

$$G(\omega) = T\,\mathrm{sinc}\left(\frac{\omega}{\omega_r}\right), \quad (34)$$

where ω_r (=2π/T) is the clock radian frequency. The frequency spectrum $G_R(\omega)$ of the received pulse at desired channel 1 is given as follows:

$$G_R(\omega) = G(\omega)\cdot H_{1\to1}(\omega)\,. \quad (35)$$

The received pulse $g_R(t)$ can be obtained by the inverse Fourier transform of $G_R(\omega)$ as follows:

$$g_R(t) = \frac{1}{16}\left\{g\left(t+\frac{3}{2}T_d\right) + 2g(t+T_d) + 3g\left(t+\frac{1}{2}T_d\right) + 4g(t) + 3g\left(t-\frac{1}{2}T_d\right) + 2g(t-T_d) + g\left(t-\frac{3}{2}T_d\right)\right\}. \quad (36)$$

Thus, the received signal can be expressed as follows:

$$g_{R1}(t) = \sum_{k=-\infty}^{\infty} a_k g_R(t - kT)\cos\omega_1 t\,. \quad (37)$$

C. Eye Pattern and Eye Aperture

Figure 4 shows the eye pattern of desired channel 1 when ω_d/ω_r $(= T/2T_d)$ is 2.0. The carrier wave is omitted here. The value of the eye aperture A_e can be obtained as follows:

$$A_e = v(2g_R(0) - 1)\,, \quad (38)$$

$$v(x) = x\cdot u(x)\,, \quad (39)$$

where $u(x)$ is a step function.

Figure 5 shows the calculated values of the eye aperture A_e as a function of ω_d/ω_r. When ω_d/ω_r is greater than 1.5, the eye is fully open. Otherwise, the degree of eye openness decreases due to inter-symbol interference. There are three discontinuous changes when $\omega_d/\omega_r = 0.5$, $\omega_d/\omega_r = 1.0$, and $\omega_d/\omega_r = 1.5$ because the pulse signal transmits under the assumption of no dispersion.

IV. Signal To Inter-Channel Interference Ratio

A. Interference Signal PSD

The signals from transmit ports 2, 3, and 4 to receive port 1 are considered to interfere with the signal from transmit port 1. As a result of incoherent transmission, the signals of $g_{T2}(t)$, $g_{T3}(t)$, and $g_{T4}(t)$ at these transmit ports are random processes and are assumed to be given as follows:

$$g_{T2}(t) = \sum_{k=-\infty}^{\infty} b_k g(t - kT + \xi_2)\cos(\omega_2 t + \phi_2), \quad (40)$$

$$g_{T3}(t) = \sum_{k=-\infty}^{\infty} c_k g(t - kT + \xi_3)\cos(\omega_3 t + \phi_3), \quad (41)$$

$$g_{T4}(t) = \sum_{k=-\infty}^{\infty} d_k g(t - kT + \xi_4)\cos(\omega_4 t + \phi_4), \quad (42)$$

where, b_k, c_k, and d_k are i.i.d. random variables that take 1 or 0, ξ_2, ξ_3, and ξ_4 are uniformly distributed over the range of $[0, T]$, and ϕ_2, ϕ_3, and ϕ_4 are uniformly distributed over the range of $[0, 2\pi]$. The power spectral densities (PSDs) of $g_{T2}(t)$, $g_{T3}(t)$, and $g_{T4}(t)$ are designated as $W_{T2}(\omega)$, $W_{T3}(\omega)$, and $W_{T4}(\omega)$, respectively, and can be given as the following equations.

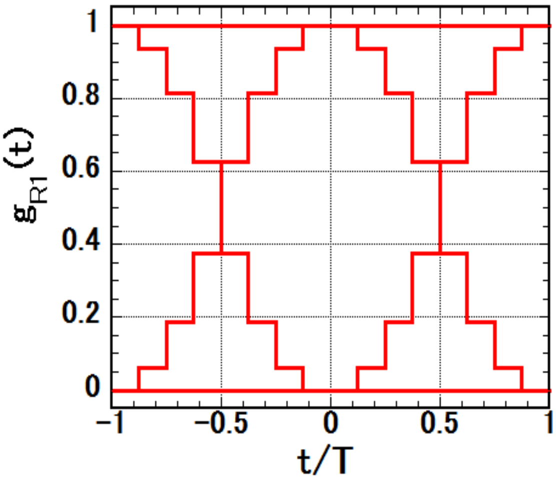

Figure 4. Eye pattern of desired channel 1.

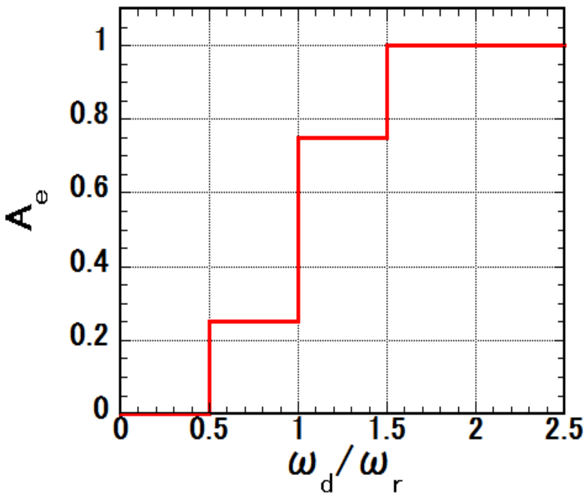

Figure 5. Eye aperture A_e.

$$W_{T2}(\omega) = \frac{1}{16T}\{|G(\omega-\omega_2)|^2 + |G(\omega+\omega_2)|^2\} + \frac{\pi}{8}\{\delta(\omega-\omega_2) + \delta(\omega+\omega_2)\}\,, \quad (43)$$

$$W_{T3}(\omega) = \frac{1}{16T}\{|G(\omega-\omega_3)|^2 + |G(\omega+\omega_3)|^2\} + \frac{\pi}{8}\{\delta(\omega-\omega_3) + \delta(\omega+\omega_3)\}\,, \quad (44)$$

$$W_{T4}(\omega) = \frac{1}{16T}\{|G(\omega-\omega_4)|^2 + |G(\omega+\omega_4)|^2\} + \frac{\pi}{8}\{\delta(\omega-\omega_4) + \delta(\omega+\omega_4)\}\,, \quad (45)$$

where $G(\omega)$ is the frequency spectrum of $g(t)$, and $\delta(\omega)$ is the Dirac delta function.

The interference signal PSDs at receive port 1 from transmit ports 2, 3, and 4 are designated as $W_{R21}(\omega)$, $W_{R31}(\omega)$, and $W_{R41}(\omega)$. The PSDs are given as follows:

$$W_{R21}(\omega) = |H_{2\to1}(\omega)|^2 W_{T2}(\omega)\,, \quad (46)$$

$$W_{R31}(\omega) = |H_{3\to1}(\omega)|^2 W_{T3}(\omega)\,, \quad (47)$$

$$W_{R41}(\omega) = |H_{4\to1}(\omega)|^2 W_{T4}(\omega)\,. \quad (48)$$

ISBN 978-89-968650-0-1

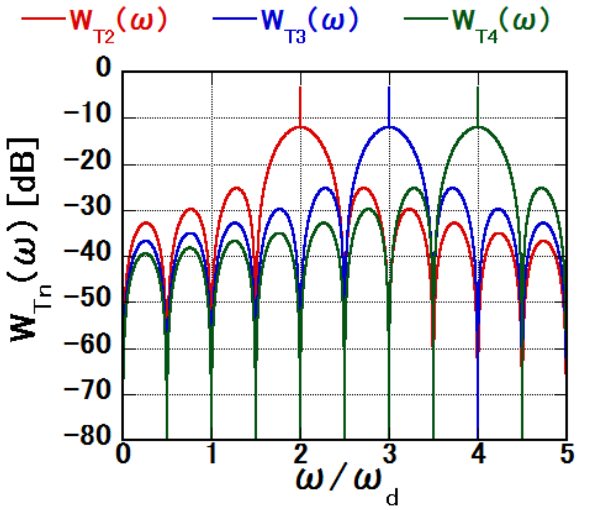

Figure 6. Transmit signal PSDs.

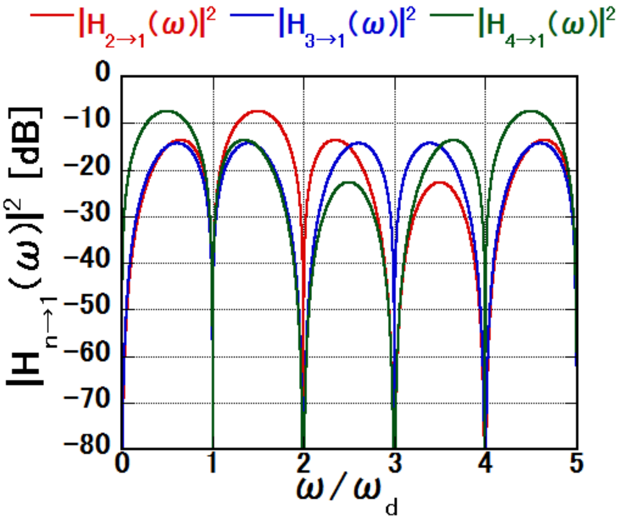

Figure 7. Transmission characteristics at the interference paths.

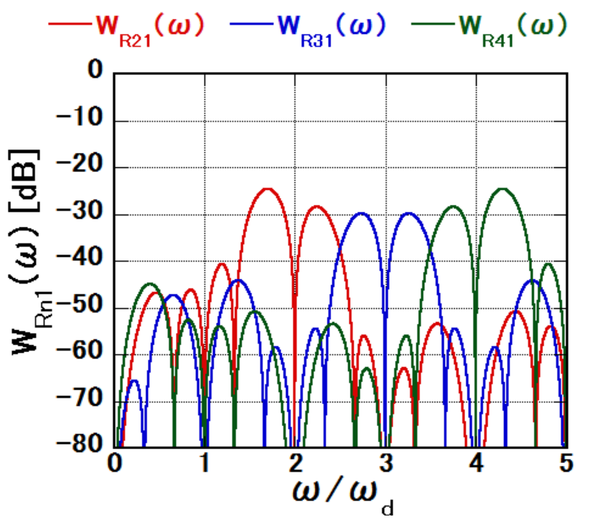

Figure 8. The interference signal PSDs at the receive port 1.

Figure 6 shows the signal PSDs at transmit ports 2, 3, and 4 as a function of ω/ω_d. Figure 7 shows the transmission characteristics $|H_{2\to1}(\omega)|^2$, $|H_{3\to1}(\omega)|^2$, and $|H_{4\to1}(\omega)|^2$ at the interference paths as a function of ω/ω_d. Figure 8 shows the interference signal PSDs at receive port 1 from transmit ports 2, 3, and 4 as a function of ω/ω_d. These PSDs can be obtained as the product of the transmit signal PSDs and the transmission characteristics, as shown in equations (46) through (48).

B. A Signal to Inter-Channel Interference Ratio

A signal to inter-channel interference ratio ρ_1 at receive port 1 for the four-channel system can be expressed as follows:

$$\rho_1 = \frac{A_e^2/2}{P_{R21}+P_{R31}+P_{R41}}, \tag{49}$$

where P_{R21}, P_{R31}, and P_{R41} are the interference powers, respectively, from transmit ports 2, 3 and 4 to receive port 1 and can be obtained as follows:

$$P_{R21} = \frac{1}{2\pi}\int_{-\infty}^{\infty} W_{R21}(\omega)\, d\omega\,, \tag{50}$$

$$P_{R31} = \frac{1}{2\pi}\int_{-\infty}^{\infty} W_{R31}(\omega)\, d\omega\,, \tag{51}$$

$$P_{R41} = \frac{1}{2\pi}\int_{-\infty}^{\infty} W_{R41}(\omega)\, d\omega\,. \tag{52}$$

The ratios at receive ports 2, 3, and 4 can be obtained in the same manner.

C. Calculated Results

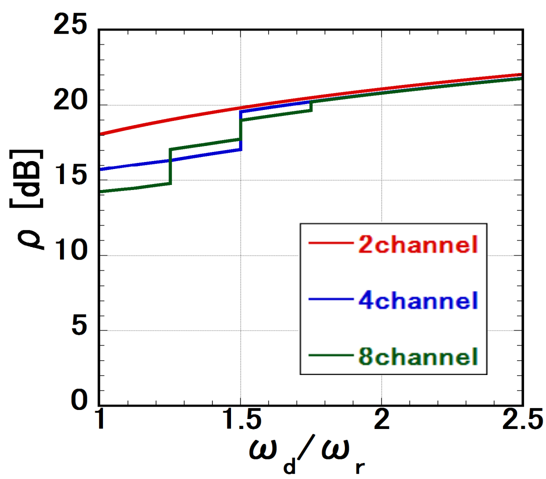

Figure 9. Signal to inter-channel interference ratio at receive port 1.

Figure 9 shows the signal to inter-channel interference ratio ρ at receive port 1 as a function of ω_d/ω_r for a two-, a four-, and an eight-channel FDM system. The signal to inter-channel interference ratio increases as ω_d/ω_r increases. This is due to the increase in channel spacing. The eye is fully open when ω_d/ω_r is greater than 1.0 in the case of the two-channel system. There are a few abrupt changes when $\omega_d/\omega_r = 1.5$ in the case of the four-channel system, and $\omega_d/\omega_r = 1.25$, 1.5, and 1.75 in the case of the eight-channel system. Abrupt changes occur at corresponding values of ω_d/ω_r, where the eye aperture A_e changes abruptly, as shown in Figure 5. These abrupt changes are caused by the pulse transmission with no dispersion assumed herein. The ratio ρ decreases due to inter-symbol interference, where ω_d/ω_r is smaller than 1.5 in the case of the four-channel system.

V. CONCLUSION

In the present paper, we applied the analysis technique of the PBF to the MZF and proposed a plain representation of the amplitude transfer function using the MZF model. Then, we presented a four-channel FDM system configuration as an example of a multi-channel FDM system, and the amplitude transfer function of the system. The calculated result of a signal to inter-channel interference ratio at desired channel 1 by applying the plain representation is shown.

As a result, although the neighboring channel spacing is desired to be as narrower as possible in order to increase the transmission capacity, the signal to inter-channel interference ratio becomes smaller and inter-symbol interference also occurs. This becomes increasingly notable as the channel number increases. Since we have assumed pulse transmission with no dispersion, the cornered eye pattern and the inter-symbol interference arise.

In future, it is expected that a transmit and receive filter will be applied to reduce the inter-symbol interference, assuming a band-limiting scheme as a cosine roll-off. Analysis of the transmission characteristics using the filters will be assumed feasible even for an FDM system that has a much larger number of channels. Experiments should be conducted in order to verify the validity of the proposed technique.

ACKNOWLEDGMENT

The authors would like to thank Professor Kazuhiro Miyauchi for his valuable guidance and support of the present research.

REFERENCES

[1] K. Miyauchi, I. Ohtomo, S. Shimada, "A transmission type periodical branching filter," *Proceedings of four electrical engineers society's joint conference (Japanese ed.)*, no.1493, pp.1769-1770, 1969.

[2] H. Kumazawa, I. Ohtomo, "30-GHz-band periodic branching filter using a traveling-wave resonator for satellite applications," *IEEE Trans. Microwave Theory Techniques*, vol.MTT-25, no.8, pp.683-687, August 1977.

[3] G. P. Agrawal, *Fiber-Optic Communication System*, Third ed., K. Chang, Ed. New York, A John Wiley & Sons, Inc., pp.123, 342, 2002.

[4] N. Takato, T. Kominato, A. Sugita, K. Jinguji, H. Toba, M. Kawachi, "Silica-based integrated optic Mach-Zehnder multi/demultiplexer family with channel spacing of 0.01-250nm," *IEEE Journal of Selected Areas in Commun*., vol.8, no.6, August 1990.

[5] T. Hanada, T. Shimoda, M. Kitamura, S. Nakamura, "FDM/WDM couplers using silica waveguide deposited by APCVD," *IEICE Trans. Electron*., vol.E80-C, no.1, pp.130-133, January 1997.

[6] K. Oda, N. Takato, H. Toba, K. Nosu, "A wide-band guided-wave periodic multi/demultiplexer with a ring resonator for optical FDM transmission systems," *IEEE Journal of Lightwave Technology*, vol.6, no.6. pp.1016-1023, June 1988.

[7] K. Nosu, H. Toba and K. Iwashita, "Optical FDM transmission technique," *IEEE Journal of Lightwave Technology*, vol.LT-5, no.9, pp.1301-1308, September 1987.

[8] K. Inoue, N. Takato, H. Toba, M. Kawachi, "A four-channel optical waveguide multi/demultiplexer for 5-GHz spaced optical FDM transmission," *IEEE Journal of Lightwave Technol.*, vol.6, no.2, pp.339-345, February 1988.

[9] S.-H. Lee, Y.-Y. Won, H.-D. Jung, S.-K. Han, "Reduction of inter-channel crosstalk using Mach-Zehnder type filter in digital/RF optical transmission link," *IEE Proc. Optoelectron.*, vol.152, no.4, pp.189-192, August 2005.

[10] B. Charbonnier, et al., "Silicon photonics for next generation FDM/FDMA PON," *J. OPT. COMMUN. NETW.*, vol.4, no.9, pp.A29-A37. September 2012.